Chemical Physics Letters 711 (2018) 166–172

Contents lists available at ScienceDirect

Chemical Physics Letters

journal homepage: www.elsevier.com/locate/cplett

Research paper

The transition state of the automerization reaction of cyclobutadiene: A theoretical approach using the Restricted Active Space Self Consistent Field method

Panayiotis C. Varras[a,*], Panagiotis S. Gritzapis[b]

[a] Department of Chemistry, University of Ioannina, 451 10 Ioannina, Greece
[b] Molecular Biology and Genetics Department, Democritus University of Thrace, University Campus, Dragana, GR-68100 Alexandroupolis, Greece

HIGHLIGHTS

- The transition state geometry for the automerization of cyclobutadiene is an isosceles trapezium.
- Enhanced π-π dynamic electron correlation is responsible.
- The calculated energy barrier is 9.62 kcal/mol (0.417 eV).

ARTICLE INFO

This paper is dedicated to our teacher, Professor Antonios K. Zarkadis (University of Ioannina, Greece).

Keywords:
Cyclobutadiene transition state
Cyclobutadiene automerization
Cyclobutadiene RASSCF

ABSTRACT

The application of the Restricted Active Space Self Consistent Field (RASSCF) quantum chemical method using an extended active space and including σ-σ, π-σ and π-π dynamical electron correlation shows that the transition state structure for the automerization reaction of cyclobutadiene is an isosceles trapezium. This transition state is obtained without any symmetry constraints. The calculated energy barrier height involving the zero point vibrational energy corrections is 9.62 kcal·mol^{-1} (0.417 eV), with the corresponding rate constant being equal to $0.18 \times 10^{9}\,s^{-1}$ (or $7.1 \times 10^{10}\,s^{-1}$ in case of using the vibrational energy splitting tunneling method).

1. Introduction

Cyclobutadiene (CBD) is a fascinating molecule that has puzzled experimental and theoretical chemists for more than 80 years [1–3]. It has been characterized as the Mona Lisa of organic chemistry [4] due to its extreme chemical instability and consequently to its fleeting existence and because it has stimulated the scientific imagination by challenging the interpretive instincts. After its synthesis in 1965 by Petit and coworkers [5], it was found that the molecule is stable in matrices at very low temperatures, usually below 35 K [6,7], and inside the cavity of a hemicarcerand [4] where it was found to be very stable for months even at room temperatures. In both cases the molecules remain far apart from each other, no other molecules can enter the cavity and thus no reaction can take place. Its ground state (S_0) structure has been proved both theoretically [8] and experimentally [9–11] to be a rectangular singlet (D_{2h} symmetry) with two alternating pairs of equal single and double bonds.

One of the most studied problems concerning cyclobutadiene is the mechanism of the automerization reaction which involves the interconversion of the two equivalent rectangular structures via a transition structure. The geometry of this transition structure, characterized by one negative frequency, is always assumed to be a perfect square of D_{4h} symmetry which is found by imposing group-symmetry restrictions and all theoretical computations involve the calculation of the height of the energy barrier (activation energy) [12–17] or the corresponding rate constant (k_r) [18–26] based either on the transition state theory and its variants with or without quantum mechanical tunneling or in vibrational energy splitting tunneling, while most of the results are within the experimental range of the energy barrier which is 1.6–10 kcal/mol (0.069–0.434 eV) [27]. However, Redington [28] in his detailed single reference wave function ab-initio molecular orbital MP2 study of state-specific vibrational anharmonicities for fast automerization in CBD describes a dilated square-planar molecular geometry which is involved in the automerization of CBD lying approximately 2 kcal/mol (0.087 eV) above the square transition state (TS) structure.

Since it is known that in the transition state the system acquires an

* Corresponding author.
E-mail address: panostch@gmail.com (P.C. Varras).

https://doi.org/10.1016/j.cplett.2018.09.028
Received 1 June 2018; Accepted 11 September 2018
Available online 18 September 2018
0009-2614/

open shell character we need more than one determinant to describe the system properly and so the use of multireference (MR) methods is mandatory for such cases, since they are well suited to represent the non-dynamic electron correlation effects. On the other hand, the dynamic electron correlation effects require a more complete treatment than that offered by the usual multireference methods.

In this paper we investigate the automerization reaction of cyclobutadiene by applying the powerful RASSCF quantum chemical method which can describe not only the non-dynamic, but also the dynamic correlation effects.

2. Computational methods

In the present study, the automerization reaction of CBD is studied in the gas phase by applying the multiconfigurational RASSCF method [29–34]. This method, which is a variant of the CASSCF (Complete Active Space Self Consistent Field), is one of the main multireference wave function methods suitable not only for the ground states but also for the excited states, capable of describing strong mixing of configurations and near degeneracy effects and depicting very well the topography of the potential energy surfaces (PESs). Additionally it has analytical first derivatives and numerical second order derivatives. CASSCF wave functions may contain a huge number of electronic configurations since inside the CASSCF active space full CI (Configuration Interaction) takes place. By choosing properly the active space for the problem under consideration, we make a partition of the initial active space into three subspaces called RAS1, RAS2 and RAS3. The RAS1 subspace contains doubly occupied orbitals and is restricted by the number of 'holes' that can enter it, or equivalently by the number of excitations into RAS2 or RAS3, while the RAS2 subspace includes the most important orbitals and inside this subspace full CI takes place. On the other hand, RAS3 contains weakly occupied or unoccupied orbitals and is defined by the number of particles, that is electrons, that can enter it. In this way, by restricting the number of excitations we reduce the initial enormous number of the CASSCF configurations making the calculation manageable.

For our problem, the active space (AS) used (Fig. 1) contains the four occupied σ_{CC} and the two occupied π orbitals as well as the corresponding unoccupied π^* and σ^*_{CC} antibonding molecular orbitals (ABMOs). Furthermore we use the diffuse $3p_\pi$ orbitals in order to capture more of the π dynamic correlation. These orbitals are partitioned in two different ways into the RAS subspaces as shown in Fig. 2. According to the first partitioning of the active space, the RAS1 subspace contains the four bonding σ_{CC} orbitals, RAS2 contains the π and π^* orbitals and RAS3 includes the four $3p_\pi$ and the four σ^*_{CC} orbitals. The total number of active electrons is therefore twelve (12) and the total number of orbitals is sixteen (16). We allow up to double excitations from RAS1 into RAS2 or RAS3 in the four (4) orbitals of RAS1 and to two electrons in the eight orbitals of the RAS3 subspace, that is electron excitations from RAS1 or RAS2 into RAS3. This active space is denoted as CASSCF(12,16,RASSCF(2,4,2,8)) or simply as RASSCF (12,4 + 4 + 8)[2,2], and produces a total number of 54,593 Configuration State Functions (CSFs). In the second partitioning of the active space we bring inside the RAS2 the four diffuse $3p_\pi$ orbitals and hence RAS2 now contains a total of eight orbitals leaving each of RAS1 and RAS3 spaces with four orbitals. The resulting subspace RAS2 is thus expanded and the new active space is now denoted as RASSCF (12,4 + 8 + 4)[2,2], and in this particular case, the total number of CSFs is 454,758.

If we allow for single excitations from RAS1 coupled with single excitations from RAS2 then we get the so called spin polarization effects [34], while by including double excitations, some dynamical correlation is being recoverd. In particular, double excitations from the σ MOs of RAS1 into the σ^* ABMOs of RAS3 gives us the σ-σ dynamical correlation, while double excitations from the π MOs of RAS2 into the π^* and the $3p_\pi$ diffuse orbitals recovers and improves further the π-π dynamic correlation. Finally, the single and double excitations from the σ orbitals of RAS1 into the π^* orbitals of RAS2 and the $3p_\pi$ orbitals of RAS3 recovers the σ-π dynamic correlation. By including dynamical electron correlation in the RASSCF method, we get very good equilibrium geometries [32,35] since it is known that the dynamic electron correlation is a function of the electron density [36].

In our calculations we used a variety of basis sets such as the 6-31G(d), 6-31 + G(d), 6-31G(d) + 3p, 6-31G(d,p) + 3p, 6-311G(d,p) + 3p and Dunning's correlation consistent cc-pVTZ basis set. It is known that all the aforementioned basis sets include the diffuse $3p_\pi$ type functions (those basis sets bearing the + sign are specially designed), however the 6-31G(d) + 3p basis set [35] uses the 3p orbitals of silicon derived from the corresponding 3p part of the 6-31G basis set of silicon with the 3p exponents scaled by a factor of 0.5. Hence, we have a specially designed basis set with not very diffuse basis functions and is as accurate as Dunning's extended aug-cc-pVDZ basis set.

Molecular geometry optimizations leading to the isosceles trapezium transition state were performed without any symmetry constraints, and for comparison purposes we have also included the square TS structure which is obtained by imposing the D_{4h} point group summetry restriction. Stationary points (minima and transition states) were optimized fully and vibrational analysis was used to confirm their nature and to provide zero-point energy (ZPE) corrections. Intrinsic Reaction Coordinate (IRC) was also used to verify the transition states and to connect reactants and products. All calculations have been carried out with the Gaussian 09 [37] software program package.

3. Results and discussion

Fig. 3 shows the equilibrium geometries of the ground state (S_0) rectangular structure of cyclobutadiene, its corresponding isosceles trapezium transition state (TS) associated with the automerization path, as well as the TS having a square geometry calculated using the larger active space and the cc-pVTZ basis set (for more details see the Electronic Supplementary Information, ESI), while Table 1 shows the optimized geometries for all basis sets used in this study.

From the numerical values of Table 1 we see that for the ground state rectangular structure and for all basis sets used except the cc-pVTZ, the single bonds (and similarly for the double bonds) differ in their length in the third decimal figure, while the use of the cc-pVTZ basis introduces a change in the bond length in the second decimal point as compared to the other basis sets. On the other hand, the optimized isosceles trapezium transition state structure obtained with any of the basis sets and with the two active spaces corresponds to an isosceles trapezium (see the ESI for a concise geometrical proof). This optimized transition state is obtained quite naturally and without any imposed symmetry constraints, since according to Houk [39], a transition structure obtained without any symmetry constraints is an authentic transition structure.

It is worth mentioning here that the isosceles trapezium structure is obtained when the diffuse $3p_\pi$ orbitals are present in the active space and only when double excitations out of RAS1 and RAS2 are used. In most other cases the square structure is obtained. For instance, by using single excitations and without any symmetry constraints the square structure is obtained. Excluding the $3p_\pi$ orbitals and allowing for double excitations the square TS is obtained again. However, if we take as an initial geometry the optimized square transition state and carry out a reoptimization using the $3p_\pi$ orbitals and double excitations we get the isosceles trapezium TS. This particular feature reminded us Coulson's remarks [40] about the important role of the π electrons, and in another study concerning the cyclobutadiene molecule [41] the large influence of the π electrons on the molecular geometry was stressed. This makes sense since by increasing the active space by using the diffuse $3p_\pi$ orbitals and taking into account the double excitations as compared to the single ones, then it is the additional improvement of the π-π and σ-π dynamical electron correlation that is important. Let us

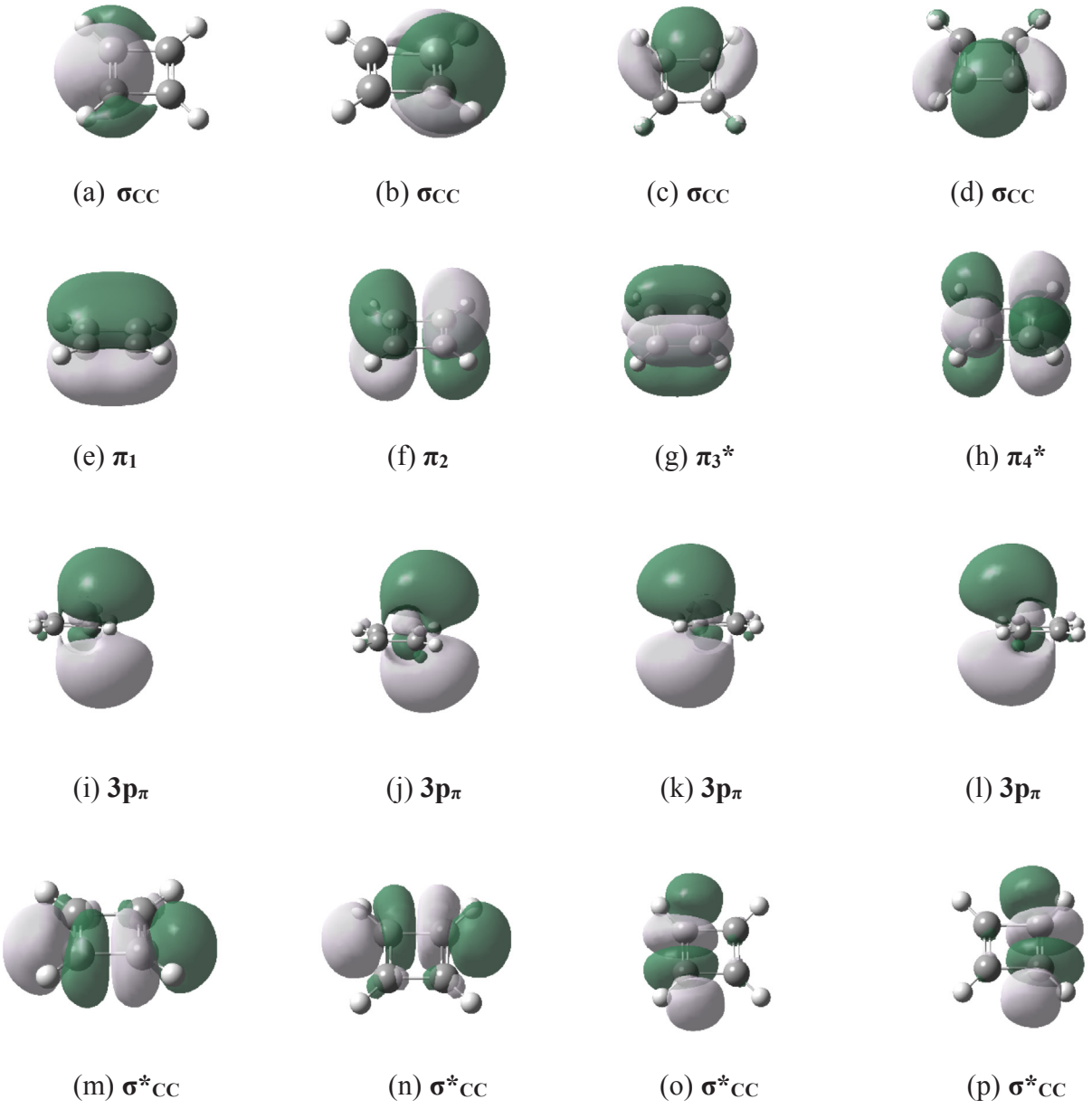

Fig. 1. The Molecular Orbitals (MOs) comprising the active space in cyclobutadiene (CBD).

now consider Fig. 4 which shows the π molecular orbital diagram for ground state rectangular CBD.

By looking at Fig. 4 we see that π_2 is the HOMO (Highest Occupied MO), π_3^* is the LUMO (Lowest Unoccupied MO) and the electronic configuration is described as $\pi_1^2\pi_2^2$. Suppose now that we compare the orbital occupancies of the optimized isosceles trapezium (IT) TS as obtained with the RAS(12,4 + 4 + 8)[2,2] active space, which includes the initial diffuse $3p_\pi$-type orbitals, with those of the optimized square TS excluding the $3p_\pi$ orbitals (RAS(12,4 + 4 + 4)[2,2]). Using the 6-31 + G(d) basis set and analyzing the electron density matrices we see that the orbital occupancies are $\pi_2^{0.94}\pi_3^{*1.11}$ for IT(TS) and $\pi_2^{0.99}\pi_3^{*0.99}$ for the square TS. Even if we use the larger active space, RAS (12,4 + 4 + 8)[2,2], and force optimization to the square TS, the orbital occupancies remain the same. Therefore we see that the π_3^* MO in the IT(TS) has ~0.12 more electrons than its corresponding counterpart in the square TS. Given the fact that the sum of all $3p_\pi$-type orbital occupancies is equal to 0.02 electrons, this means an enhanced π-π dynamic electron correlation for the first case which is reflected into the molecular geometry shape of the IT(TS) since as is well known [42] the orbital occupation numbers change with the molecular geometry.

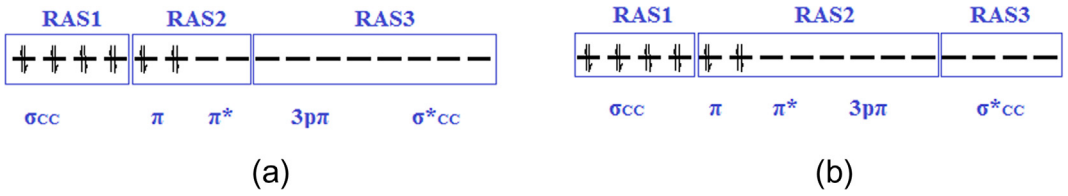

Fig. 2. The two active spaces used in this study. (a) RASSCF(12,4 + 4 + 8)[2,2], (b) RASSCF(12,4 + 8 + 4)[2,2].

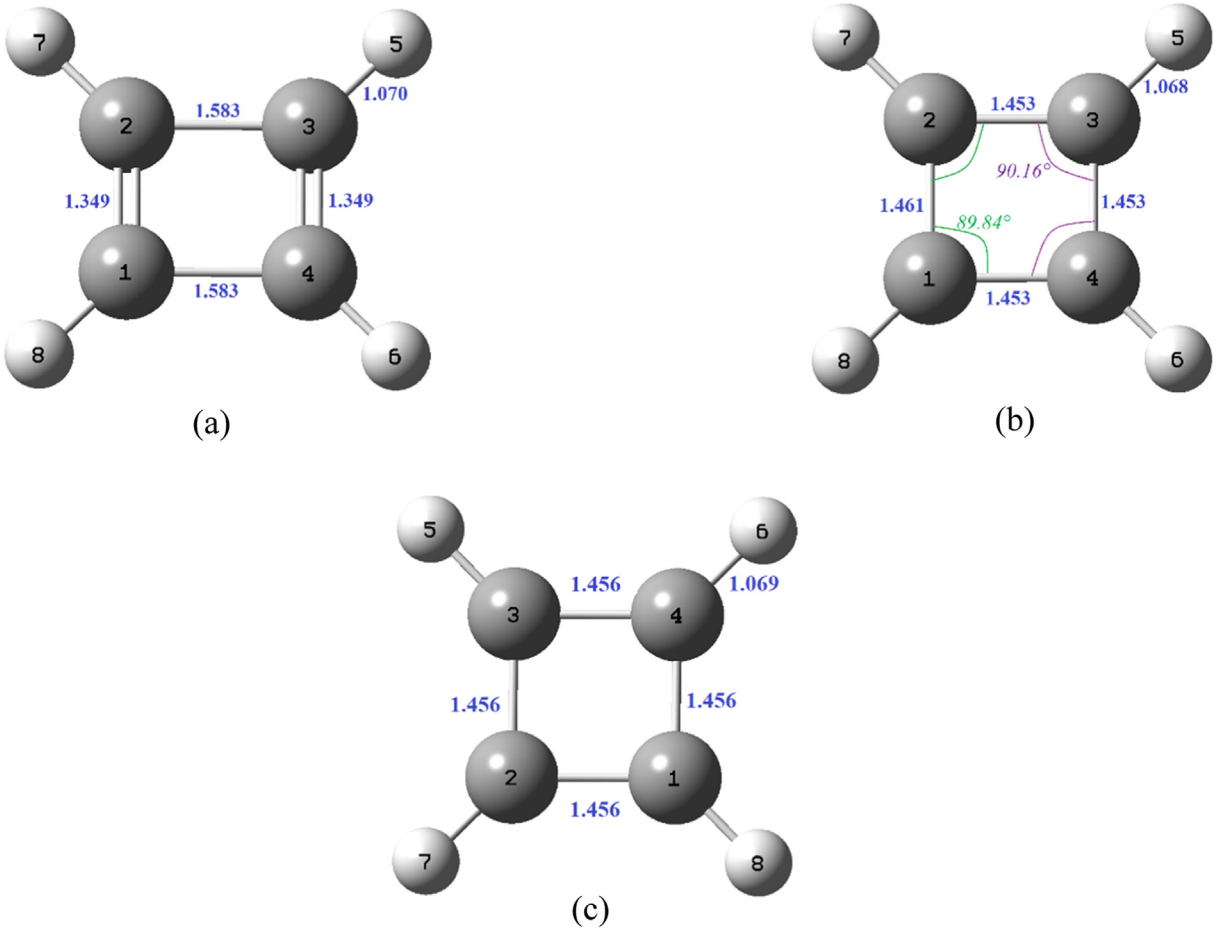

Fig. 3. RASSCF(12,4 + 8 + 4)[2,2]/cc-pVTZ equilibrium structures of (a) ground state rectangular CBD, (b) isosceles trapezium transition state (TS) and (c) Square TS. Bond lengths in angstroms (Å).

Similar remarks hold for the other basis sets too. Consequently we deduce that the IT(TS) structure has a biradicaloid character.

In an ideal situation, as cyclobutadiene is distorted from its ground state rectangular structure towards the square (D_{4h}) geometry, the HOMO-LUMO gap gets smaller and smaller until the square geometry is reached where the gap is nil [43]. In the IT(TS) geometry the gap is certainly very small but in any case it is different from zero and the distortion of the TS from D_{4h} to a lower symmetry may be due to a pseudo Jahn-Teller distortion, something which is consistent with the fact that "stability and orbital degeneracy are simultaneously incompatible unless a molecule is linear" [40].

Fig. 5a shows the IRC calculation which connects the two equivalent CBD minima on the potential energy surface (PES) by a path that passes through the IT(TS) between them, while in Fig. 5b we see the normal vibrational mode corresponding to the imaginary frequency whose value, as calculated with the RAS(4 + 4 + 8)[2,2] active space and the cc-pVTZ basis set is $\nu^{\neq} = 1794.16i\,\mathrm{cm}^{-1}$

The value of the imaginary frequency is large and the direction of the normal mode vectors shows movement towards ground state CBD.

For the calculation of the corresponding rate constants (k_r) and lifetimes (τ) we use the classical Eyring's equation (1),

$$k_r = \kappa \frac{k_B T}{h} \exp\left(\frac{-\Delta G^{\neq}}{RT}\right) \tag{1}$$

In Eq. (1) k_B is Boltzmann's constant, T is the absolute temperature, R the universal gas constant, $\Delta G^{\neq}$ is the activation free energy, h is Planck's constant and κ is the quantum mechanical tunneling coefficient which will be calculated in two different ways. In the first method we use Bell's equation [44], defined below as,

$$\kappa = \frac{\left(\frac{h\nu^{\neq}}{2k_B T}\right)}{\sin\left(\frac{h\nu^{\neq}}{2k_B T}\right)} - \frac{E_a \exp\left(\frac{E_a}{k_B T} - \frac{E_a}{h\nu^{\neq}}\right)}{\left(\frac{E_a k_B T}{h\nu^{\neq}} - E_a\right)} \times \left[1 - \sum_{n=0}^{\infty} \frac{(-1)^{n+2}\left(\frac{E_a}{h\nu^{\neq}} - \frac{E_a}{k_B T}\right) e^{-(n+1)E_a/h\nu^{\neq}}}{\left[\frac{(n+2)E_a}{h\nu^{\neq}} - \frac{E_a}{k_B T}\right]}\right] \tag{2}$$

In Eq. (2), $\nu^{\neq}$ is the imaginary frequency at the transition state associated with the reaction coordinate and E_a is the activation energy. In the second method we use the Skodje-Truhlar equation [45] which is a generalization of Bell's equation applied to parabolic potential barriers and is defined as follows,

$$\kappa = \sum_{n=0}^{\infty} (-1)^n \beta \left[\frac{1 - e^{[\beta - (n+1)\alpha]\cdot E_a}}{(n+1)\alpha - \beta} + \frac{1}{n\alpha + \beta}\right] \tag{3}$$

The parameters α and β are defined through the following relations:

$$\alpha = \frac{2\pi}{h\,\mathrm{Im}(\nu^{\neq})}, \qquad \beta = \frac{1}{k_B T} \tag{4}$$

The notation $\mathrm{Im}(\nu^{\neq})$ means the imaginary part of the frequency which is always a real number. Both infinite series defined in Eqs. (2) and (3) are fully convergent (see the ESI for the corresponding mathematical proofs). We must also note here that both methods give practically the same results.

As a third approximation to the calculation of the rate constant for the automerization reaction of CBD we use the method of vibrational

Table 1
Selected geometrical parameters for ground state, rectangular, CBD and its isosceles trapezium and square transition states. Bond lengths (r) are given in angstroms (Å), to within three (significant) decimal figures according to the suggestions of Hoffmann, Schleyer and Shaefer [38] and *PG* is the corresponding molecular point group (see ESI).

Active space: RASSCF(12,4 + 4 + 8)[2,2]

PG	r_{C1C2}	r_{C2C3}	r_{C3C4}	r_{C1C4}	r_{C-H}	*Basis set*
Ground state (Rectangle)						
D_{2h}	1.356	1.583	1.356	1.583	1.072	6-31G(d)
D_{2h}	1.358	1.582	1.358	1.582	1.072	6-31 + G(d)
D_{2h}	1.358	1.583	1.358	1.583	1.072	6-31G(d) + 3p
D_{2h}	1.358	1.583	1.358	1.583	1.072	6-31G(d,p) + 3p
D_{2h}	1.357	1.584	1.357	1.584	1.072	6-311G(d,p) + 3p
D_{2h}	1.349	1.583	1.349	1.583	1.070	cc-pVTZ
Transition State (TS) [Isosceles Trapezium]						
C_{2v}	1.467	1.454	1.457	1.454	1.070	6-31G(d)
C_{2v}	1.469	1.454	1.459	1.454	1.070	6-31 + G(d)
C_{2v}	1.469	1.454	1.459	1.454	1.070	6-31G(d) + 3p
C_{2v}	1.469	1.454	1.459	1.454	1.070	6-31G(d,p) + 3p
D_{2h}	1.466	1.456	1.458	1.456	1.070	6-311G(d,p) + 3p
D_{2h}	1.461	1.453	1.453	1.453	1.068	cc-pVTZ
Transition State (TS) [Square]						
D_{4h}	1.459	1.459	1.459	1.459	1.071	6-31G(d)
D_{4h}	1.459	1.459	1.459	1.459	1.071	6-31 + G(d)
D_{4h}	1.459	1.459	1.459	1.459	1.071	6-31G(d) + 3p
D_{4h}	1.459	1.459	1.459	1.459	1.071	6-31G(d,p) + 3p
D_{4h}	1.459	1.459	1.459	1.459	1.071	6-311G(d,p) + 3p
D_{4h}	1.456	1.456	1.456	1.456	1.069	cc-pVTZ

Active space: RASSCF(12,4 + 8 + 4)[2,2]

	r_{C1C2}	r_{C2C3}	r_{C3C4}	r_{C1C4}	r_{C-H}	*Basis set*
Ground state (Rectangle)						
D_{2h}	1.349	1.583	1.349	1.583	1.070	cc-pVTZ
Transition State (TS) [Isosceles Trapezium]						
D_{2h}	1.461	1.453	1.453	1.453	1.068	cc-pVTZ
Transition State (TS) [Square]						
D_{4h}	1.456	1.456	1.456	1.456	1.069	cc-pVTZ

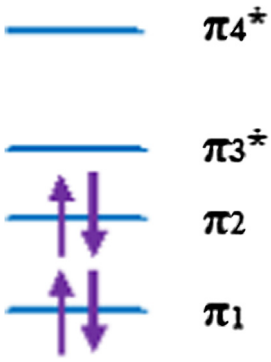

Fig. 4. The π-MO energy levels for ground state rectangular CBD.

energy splitting tunneling [21–24] which considers one dimensional tunneling through a symmetric double minimum potential in terms of the vibrational energy splitting of the corresponding ground state reactive normal mode of vibration, ν_F. It has been found [21] that most of the effective tunneling in this case arises mainly from the vibrational ground state (v = 0) since even at room temperature $k_BT/hc \sim 200\,cm^{-1}$, and all the calculated vibrational wave numbers are greater than $200\,cm^{-1}$ and consequently according to the Boltzmann distribution theorem the majority of the molecules will be in the vibrational ground states. In this case the rate constant is related to the vibrational energy splitting, ΔE_{split}, through Eq. (5),

$$k_r = \frac{2\Delta E_{split}}{h} \tag{5}$$

where the vibrational energy splitting is further defined through the following equations,

$$\Delta E_{split} = \frac{h\nu_F}{\pi} e^{-\vartheta} \tag{6}$$

$$\vartheta = \frac{[E_a - \sqrt{E_a E'_0}]}{\hbar\nu^{\neq}} \tag{7}$$

$$E'_0 = \frac{h\nu_F}{2} \tag{8}$$

We find that $\Delta E_{split} = 1.18–1.2\,cm^{-1}$ using the large RAS(4 + 8 + 4)[2,2] active space and the cc-pVTZ basis set given that $\nu_F = 1566.55\,cm^{-1} = 4.69639{\cdot}10^{13}\,s^{-1}$. In Table 2, we report the calculated values of the rate constants and life times for all basis sets used in this study along with their corresponding active spaces as well as the activation energies and activation free energies.

By looking at the numerical values of Table 2 we see that the activation energy (E_a) concerning the IT(TS) varies from 8.50 to 9.62 kcal/mol, while that for the square TS spans a range between 6.8 up to 8.5 kcal/mol, implying that the square TS is slightly energetically lower compared to that of the IT(TS) from 0.5 to 1.8 kcal/mol, something which is in a very good agreement with Redington's predictions [28]. At this point we should like to emphasize that by introducing dynamic correlation, all the aforementioned RASSCF calculations point towards an isosceles trapezium TS. However, it is known [46] that we cannot prove that a transition state does not exist and possibly only quantum dynamics calculations can resolve this issue. Consequently, we may assume that both transition states, the IT(TS) and the square TS coexist on the potential energy hypersurface.

All the calculated RASSCF activation energies are within the experimental energy range. Introducing quantum mechanical tunneling the rate constants increase by an order or two orders of magnitude depending on the particular basis set used. On the other hand, the use of the vibrational energy splitting tunneling method increases the value of the rate constant still further by an order of magnitude. This is a fact which is well known in the scientific literature [24] and much discussion has been devoted in this topic. We must however emphasize at this point that the automerization reaction of CBD is a bond stretching/compression event (Fig. 3) aided by the phenomenon of quantum mechanical tunneling since given the fact that the average change in the CC distance, that is the distance the carbon atoms move along the reaction coordinate, is $\delta_{CC} \sim 0.1$ Å, then for a kinetic energy corresponding to the barrier height $E_k = 9.62$ kcal/mol = 6.6838×10^{-23} KJ/atom, we find that the wavelength is $\lambda = h/p = 0.182$ Å. Hence, the aforementioned change in the distance between the carbon atoms is of the order of the de Broglie wavelength of the carbon atom, signaling the significance of quantum mechanical tunneling [47].

4. Conclusions

In this study concerning the famous automerization reaction of cyclobutadiene, the application of the RASSCF method using an extended active space incorporating diffuse orbitals of $3p_\pi$ type and the inclusion of dynamic correlation shows that the transition state structure is an isosceles trapezium. This transition state is obtained without any symmetry restrictions. We believe that this is an attribute of the enhanced π-π dynamic electron correlation showing that sometimes nature surprises us by using paths guided by special quantum phenomena. The predicted energy barrier is 9.62 kcal/mol (0.417 eV).

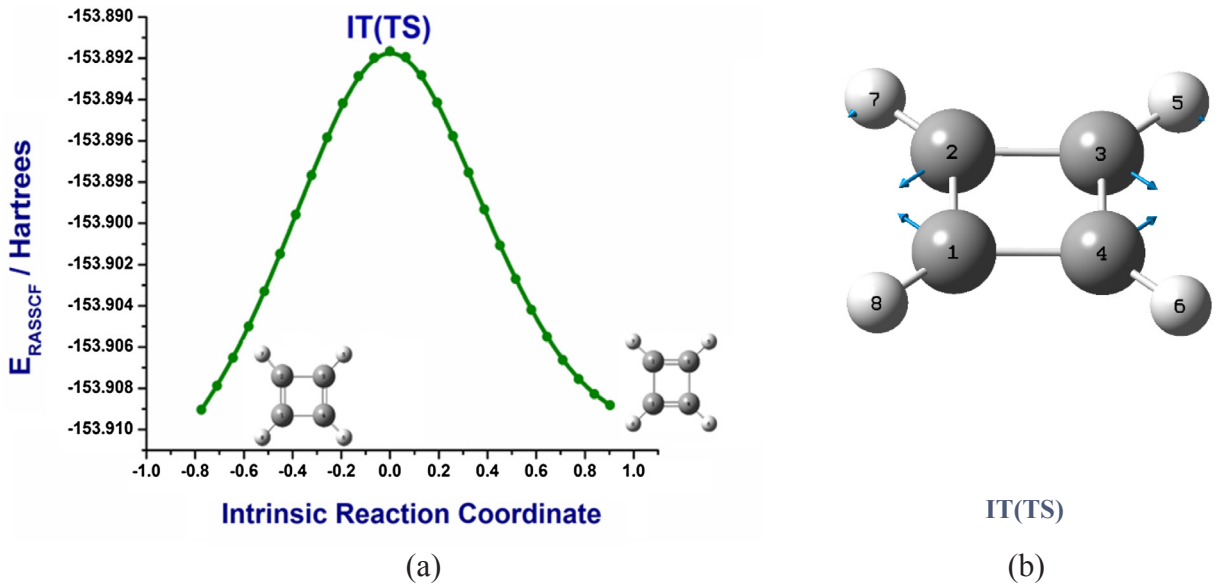

Fig. 5. (a) IRC path from the isosceles trapezium transition state, IT(TS) and (b) the corresponding normal mode of vibration. (Calculation method RAS(4 + 4 + 8) [2,2]/cc-pVTZ).

Table 2
Calculated activation energies (E_a/kcal·mol^{-1}) including the ZPE corrections, rate constants (k_r/s^{-1}) and life-times (τ/ns) for the automerization reaction of cyclobutadiene.

Geometry	$^{\alpha}E_a$/kcal·mol^{-1}	k_r/s^{-1}	τ/ns	$k_r^{(tunneling)}$/s^{-1}	$\tau^{(tunneling)}$/ns	Basis set
Active space: RASSCF(12,4 + 4 + 8)[2,2], {54,593 CSFs}						
Isosceles trapezium	7.9	0.10×10^8	100	0.61×10^9	1.64	6-31G(d)
Square	7.0	0.46×10^8	21.7	1.84×10^9	0.54	6-31G(d)
Isosceles trapezium	8.56	0.33×10^7	303	0.32×10^9	3.13	6–31 + G(d)
Square	7.7	0.14×10^8	71.4	1.03×10^9	0.97	6–31 + G(d)
Isosceles trapezium	8.77	0.23×10^7	435	0.26×10^9	3.78	6-31G(d) + 3p
Square	8.10	0.72×10^7	138.9	0.63×10^9	1.59	6-31G(d) + 3p
Isosceles trapezium	8.5	0.37×10^7	270	0.37×10^9	2.70	6-31G(d,p) + 3p
Square	8.0	0.85×10^7	117	0.70×10^9	1.43	6-31G(d,p) + 3p
Isosceles trapezium	8.5	0.37×10^7	270	0.55×10^9	1.80	6-311G(d,p) + 3p
Square	6.8	0.64×10^8	15.6	3.92×10^9	0.26	6-311G(d,p) + 3p
Isosceles trapezium	9.0	0.16×10^7	625	0.37×10^9	2.70	cc-pVTZ
Square	8.5	0.37×10^7	270	0.56×10^9	1.79	cc-pVTZ
Active space: RASSCF(12,4 + 8 + 4)[2,2], {454,758 CSFs}						
Isosceles trapezium	9.62	0.55×10^6	1820	0.18×10^8	5.56	cc-pVTZ
Square	7.81	0.14×10^8	71.4	1.58×10^9	0.63	cc-pVTZ
Vibrational Energy Splitting Tunneling						
Isosceles trapezium	9.62			7.1×10^{10}	0.0141 (14.1 ps)	cc-pVTZ
Square	7.81			3.2×10^{11}	0.003 (3.13 ps)	cc-pVTZ
$^{\beta}$Experimental	1.6–10					

α. In all cases $\Delta G^{\neq} = E_a$, β. Ref [27].

Acknowledgments

We would like to thank the mathematician Mr. Lampros Zacharakis for his elegant and concise geometrical proof concerning the isosceles trapezium quoted in the Electronic Supplementary Information and Prof. Konstantinos Skobridis (Univ. of Ioannina, Chemistry Department) for exciting discussions.

Appendix A. Supplementary material

Supplementary data to this article can be found online at https://doi.org/10.1016/j.cplett.2018.09.028.

References

[1] T. Bally, S. Masamune, Tetrahedron 36 (1980) 343.
[2] G. Maier, Angew. Chem. Int. Ed. Engl. 27 (1988) 309.
[3] T. Bally, Angew. Chem. Int. Ed. 45 (2006) 6616.
[4] H. Dodziuk, Short-lived Species Stabilized in "Molecular" or "Supramolecular Flasks", in: H. Dodziuk (Ed.), Strained Hydrocarbons: Beyond the van't Hoff and Le Bel Hypothesis, Wiley-VCH, Verlag GmbH & Co. KGaA, Weinheim, 2009, pp. 449–452.
[5] L. Watts, J.D. Fitzpatrik, R. Pettit, J. Am. Chem. Soc. 87 (1965) 3253.
[6] J. March, Advanced Organic Chemistry: Reactions, Mechanisms and Structure, Second ed, McGraw-Hill, 1977.
[7] T.H. Lowry, K.S. Richardson, Mechanism and Theory in Organic Chemistry, Harper and Row, 1976.
[8] H. Kollmar, V. Staemmler, J. Am. Chem. Soc. 99 (1977) 3583.
[9] O. Ermer, E. Heilbronner, Angew. Chem. Int. Ed. Engl. 22 (1983) 402.
[10] H. Irngartiner, M. Nixdorf, Angew. Chem. Int. Ed. Engl. 22 (1983) 403.
[11] J. Kreile, N. Münzel, A. Schweig, H. Specht, Chem. Phys. Lett. 124 (1986) 140.
[12] G. Maier, R. Wolf, H.O. Kalinowski, Angew. Chem. Int. Ed. Engl. 31 (1992) 738.
[13] M. Eckert-Maksić, M. Vazdar, M. Barbatti, H. Lischka, Z.B. Maksić, J. Chem. Phys. 125 (2006) 64310.
[14] O. Demel, J. Pittner, J. Chem. Phys. 124 (2006) 144112.
[15] P.B. Karadakov, J. Phys. Chem. A 112 (2008) 7303.
[16] T. Saito, S. Nishihara, Y. Kitigawa, T. Kawakami, S. Yamanaka, M. Okumura,

K. Yamaguchi, Chem. Phys. Lett. 498 (2010) 253.
[17] D.I. Lyakh, V.F. Lotrich, R.J. Bartlett, Chem. Phys. Lett. 501 (2011) 166.
[18] B.K. Carpenter, J. Am. Chem. Soc. 105 (1983) 1700.
[19] S. Kozuch, RSC Adv. 4 (2014) 21650.
[20] S. Kozuch, Electronic Supplementary Material (to ref. 19) for RSC Advances, 2014.
[21] M.J. Huang, M. Wolfsberg, J. Am. Chem. Soc. 106 (1984) 4039.
[22] M.J.S. Dewar, K.M. Merz Jr., J.J.P. Stewart, J. Am. Chem. Soc. 106 (1984) 4040.
[23] P. Carsky, R.J. Bartlett, G. Fitzerald, J. Noga, V. Spirko, J. Chem. Phys. 89 (1988) 3008.
[24] R. Lefebvre, N. Moiseyev, J. Am. Chem. Soc. 112 (1990) 5052.
[25] P. Carsky, J. Michl, Theor. Chim. Acta 84 (1992) 125.
[26] C. Mediavilla, J. Tortajada, V.G. Baonza, Chem. Phys. Lett. 454 (2008) 387.
[27] D.W. Whitman, B.K. Carpenter, J. Am. Chem. Soc. 104 (1982) 6473.
[28] R.L. Redington, J. Chem. Phys. 109 (1998) 10781.
[29] B. Roos, R. Lindh, P.A. Malmqvist, V. Veryazov, Per-Olaf Widmark, Multiconfigurational Quantum Chemistry, Wiley, New Jersey, 2016.
[30] J. Olsen, B.O. Roos, P. Jørgensen, H.J.A. Jensen, J. Chem. Phys. 89 (1988) 2185.
[31] M. Klene, M.A. Robb, L. Blancafort, M.J. Frisch, J. Chem. Phys. 119 (2003) 713.
[32] S. Li, Developments of Algorithms for the direct Multiconfigurational Self-Consistent (MCSCF) Method, PhD Thesis Department of Chemistry, Imperial College, London, UK, 2011.
[33] F. Krausbeck, D. Mendive-Tapia, A.J.W. Thom, M.J. Bearpark, Comput. Theor. Chem. 1040–1041 (2014) 14.
[34] V. Santolini, J.P. Malhado, M.A. Robb, M. Garavelli, M.J. Bearpark, Mol. Phys. 113 (2015) 1978.
[35] M. Boggio-Pasqua, M.J. Bearpark, M. Klene, M.A. Robb, J. Chem. Phys. 120 (2004) 7849.
[36] L. Blancafort, F. Ogliaro, M. Olivucci, M.A. Robb, M.J. Bearpark, A. Sinicropi, Computational Investigation of Photochemical Reaction Mechanisms, in: A.G. Kutateladze (Ed.), Computational Methods in Photochemistry, Taylor and Francis, New-York, 2005, p. 43.
[37] M. J. Frisch, G. W. Trucks, H. B. Schlegel, et al., Gaussian 09, Revision B.01 (Gauss Inc., Wallingford, CT, 2010).
[38] R. Hoffmann, P. von, R. Schleyer, H.F. Shaefer III, Angew. Chem. Int. Ed. 47 (2008) 7164.
[39] Y. Li, K.N. Houk, J. Am. Chem. Soc. 118 (1996) 880.
[40] C.A. Coulson, W.E. Moffitt, Phil. Mag. 40 (1948) 1.
[41] F. Dijkstra, J.H. Van Lenthe, R.W.A. Havenith, L.W. Jenneskens, Int. J. Quantum Chem. 91 (2003) 566.
[42] V. Veryazov, P.A. Malmqvist, B.O. Roos, Int. J. Quant. Chem. 111 (2011) 3329.
[43] S.M. Bachrach, Computational Organic Chemistry, Wiley-Interscience, New Jersey, 2007, p. 18.
[44] V.H. Carvalho-Silva, V. Aquilanti, H.C.B. de Oliveira, K.C. Mundim, J. Comput. Chem. 38 (2017) 178.
[45] R.T. Skodje, D.G. Truhlar, J. Phys. Chem. 85 (1981) 624.
[46] F. Jensen, Introduction to Computational Chemistry, Second ed., Wiley, 2007, p. 405.
[47] R.P. Bell, The Tunnel Effect in Chemistry, Chapman and Hall, London, 1980.